university of groningen

University Medical Center Groningen

University of Groningen

Electron spin transport in graphene and carbon nanotubes

Tombros, Nikolaos

IMPORTANT NOTE: You are advised to consult the publisher's version (publisher's PDF) if you wish to cite from it. Please check the document version below.

Document Version
Publisher's PDF, also known as Version of record

Publication date:
2008

Link to publication in University of Groningen/UMCG research database

Citation for published version (APA):
Tombros, N. (2008). *Electron spin transport in graphene and carbon nanotubes*. s.n.

Copyright
Other than for strictly personal use, it is not permitted to download or to forward/distribute the text or part of it without the consent of the author(s) and/or copyright holder(s), unless the work is under an open content license (like Creative Commons).

Take-down policy
If you believe that this document breaches copyright please contact us providing details, and we will remove access to the work immediately and investigate your claim.

Downloaded from the University of Groningen/UMCG research database (Pure): http://www.rug.nl/research/portal. For technical reasons the number of authors shown on this cover page is limited to 10 maximum.

Download date: 17-01-2021

3

Experimental techniques

This chapter presents the fabrication techniques used for the production of graphene (or carbon nanotube) based spintronic devices and of tin nanowire based superconducting devices. I present the technologies used to characterize the graphene layers, which are optical microscopy, atomic force microscopy and Raman spectroscopy. I present some ideas how to produce graphene layers on different substrates and how to produce a free standing graphene layer on a polymer layer. I conclude with the electrical characterization setups.

3.1 Electron Beam Lithography

The largest dimension of the material which we investigate in the experiments reported in this thesis, is in the micro meter range. For example, the single-walled nanotubes have a length usually smaller than 4 μm, the graphene flakes are not larger than 30 μm and the tin nanowires encapsulated in a multi-walled carbon nanotube not longer than 3 μm. To produce electrical contacts on those systems we use electron beam lithography in all cases.

Electron Beam Lithography (EBL) is a very flexible method to produce an electrical device on a substrate [1,2]. A polymer, polymethylmethacrylate (PMMA), diluted in a solvent, is spin coated on the substrate and annealed in the oven. By this the solvent is removed with final result a homogeneous solid thin film of polymer on the substrate (Fig. 3.1). When an area is exposed to a dose of accelerated electrons (usually 10 to 100 keV), the polymer fragments into very small parts. This exposed polymer can be removed using a mixture of methylisobutylketone (MIBK) and isopropanol (IPA) with a ratio of 1 to 3, in what is called the development step. During the development step, which usually does not take more than several minutes, the unexposed polymer is not affected and is used as a mask. If now we evaporate a material, for example cobalt which is a ferromagnet, then the cobalt sticks on the substrate at the places where the developer removed the exposed PMMA. The cobalt which sticks on the unexposed PMMA (mask) can be removed from the sample by dissolving the polymer in hot acetone, this is called the lift-off step. The result is a clean sample with cobalt structures only at places where we exposed the PMMA with an electron beam.

There are different types of PMMA and only a limited amount give high resolution EBL structures. One example is the high molecular weight PMMA 950K which we also use in our group. This polymer is usually diluted in chlorobenzene and lately can also be found commercially as a polymer diluted in ethyllactat-n-Butylacetat (from ALLRESIST GmbH). There are two reasons why we prefer not to use chlorobenzene, first of all it is hazardous for health. Second, we have observed that chlorobenzene strongly reacts with cobalt electrodes. Anicole is the best substitute, it causes no hazard and does not react with cobalt.

3.2 Fabrication steps

We present the fabrication of the devices discussed in this thesis. We start with a very crucial part, the fabrication of gold markers on a SiO_2 substrate which is a common step for all types of devices (nanotube, graphene and tin nanowires based). Afterwards we present the fabrication procedure for each device. We note that the goal is to obtain a substrate containing as many as possible candidates

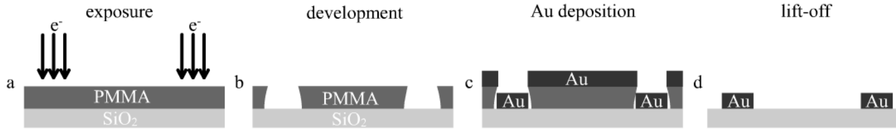

Figure 3.1: Example of an electron beam lithography process. a)A thin poly-methylmethacrylate (PMMA) layer is exposed with highly energetic electrons (10-100keV) b)Development in MIBK/IPA results to a PMMA mask c) The evaporated gold (Au) sticks on the SiO_2 layer and on the PMMA d) Lift-off in hot aceton results to the removal of the PMMA mask and the gold covering it.

(SWNT's/graphene/Sn wires) for producing a spintronic (or electronic) device. The yield of working devices can be very different for different type of devices, for example graphene devices have a yield of about 50% and Sn nanowire devices about 15% and therefore it is preferred to make a larger amount of devices on a single substrate to be able to perform spintronic (or electronic) measurements on at least one working device. For Sn wire devices this would ask for at least 8 devices and for graphene a minimum of two on a substrate.

3.2.1 Markers

Before fabrication of the device, it is crucial to know the exact position of the material under investigation, for example a graphene flake, on the substrate. For this, using EBL, we cover a large part of a silicon oxide piece with small ($\sim$ 200 x 200nm^2) gold markers equally spaced by 14 μm distance from each other (Fig. 3.2). After this we put the material under investigation, for example graphene, on the gold patterned substrate. Our preparation technique gives about 15 good quality graphene flakes on an area of 1 cm^2. Since this area contains gold markers, we are able to define the relative position of each graphene flake to a nearby gold marker within an accuracy of 50 nm (Fig. 3.2) using an atomic force microscope. A recipe for producing the markers is given in appendix B.

3.2.2 Fabrication of a single-walled carbon nanotube device

The next steps are needed for the preparation of a single wall carbon nanotube spintronic device.

1)Preparation of a SWNT suspension in chlorobenzene

The material we use contains about 90% single-walled nanotubes, (SWNTs) the remaining 10% contains catalytic particles and amorphous carbon. Due to van

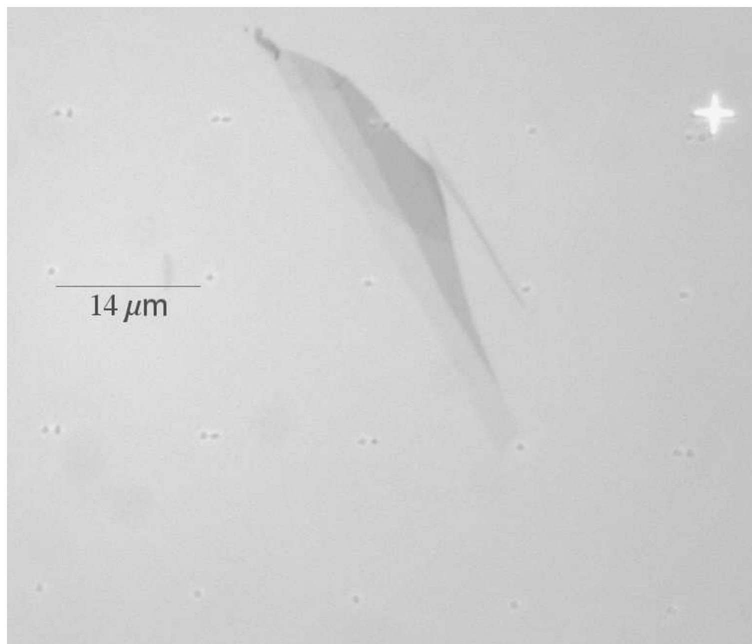

Figure 3.2: Optical image of a SiO_2 substrate covered with gold markers and a piece of HOPG graphite. The gold markers are separated by a distance of 14 μm. The position of the graphite layers with respect to the markers is known with a precision of 50 nm.

der Waals forces the single wall nanotubes attach to each other and form bundles. To separate them, we ultrasonicate (100 W for 10 min) the raw material in chlorobenzene. Chlorobenzene is hazardous for health, however, we found that it is the best solvent to reduce the number of nanotube bundles. We use 1 mg of raw material in 100 ml chlorobenzene.

2)Preparation of gold markers on a SiO_2 surface

The markers are produced on a Si-SiO_2 substrate (from Silicon Quest International) using electron beam lithography. The Si is highly doped (n, 0.0015-0.007 Ωcm) and the SiO_2 has a thickness of 500 nm.

3)Cleaning of the SiO_2 surface using oxygen plasma etching

The Si-SiO_2 substrate not only contains gold markers but is also contaminated with PMMA remains. We remove the organic remains using oxygen plasma etching (time: 3 minutes, power: 40W, O_2 flow: 9 sccm, pressure: 9 mbar).

4)Deposition of SWNTs using the dielectrophoresis technique

Deposition of a droplet of the carbon nanotube suspension on the SiO_2 and blowing it dry with nitrogen gas results in a surface containing a small number of SWNTs and a large number of large amorphous carbon particles and SWNT bundles. The method we use to obtain a surface containing only SWNTs and a small amount of bundles is dielectophoresis [3]. Here the application of a Mhz ac voltage modulation on two metallic electrodes inside the SWNT-chorobenzene suspension attracts the SWNTs to the electrodes by the dielectophoresis force. In this case the number of SWNTs at the area around the electrodes is far higher compared to all other particles such as catalytic particles, amorphous carbon particles and large SWNT bundles.

5)Atomic force microscopy

We use atomic force microscopy (AFM) in tapping mode (NanoScope IV from Digital Instruments, Veeco Metrology Group) to select the nanotubes for the fabrication of an spintronic device. Here we select nanotubes with a diameter not larger than 3 nm. When this diameter exceeds this value then it is usually a multi-walled nanotube or a bundle of nanotubes. An AFM picture should contain the carbon nanotube we would like to contact and at least one gold marker. In this case we can define with high precision the position of a nanotube with respect to the marker.

6)Electron beam lithography

We spin PMMA 950K (2% in ethyllactat-n-Butylacetat, AR-P 679.02 from ALL-RESIST GmbH, thickness: 70 nm at 4000 RPM spinning) in such a way as to obtain a 140 nm thick polymer layer (spin the PMMA on the sample at 4000 RPM, annealed it for 20 min and then spin one more time at 4000 RPM, the total thickness is then approximately 140 nm) and annealed it for at least one hour to remove the solvent. Using EBL we define the contacts (A recipe for producing the contacts is given in appendix *B*)

7)Evaporation of cobalt and lift off

We evaporate 50 nm of cobalt (e-gun evaporation, Temescal) at a rate of 0.2 nm/s and at a pressure of $\sim$5 10^{-7} mbar. Lift off is done in warm acetone at a temperature of about 30 ^{o}C. Afterwards we clean up the sample in IPA and blow it dry using nitrogen gas.

8)Bonding

We glue the sample to a chip carrier. Connection between the samples and the sample holders is made using ultrasonic wire bonding. The sample is ready for measurements.

3.2.3 Fabrication of a Sn nanowire device for superconducting measurements

For the preparation of a tin nanowire device we follow the next steps:

1)Preparation of a Sn nanowire suspension in chlorobenzene

The majority of the raw material contains tin nanowires encapsulated in multi-walled nanotubes [4]. We make a suspension in chlorobenzene en ultrasonicate it to produce a suspension containing a small amount of nanotube bundles.

2)Preparation of gold markers on a SiO_2 surface

The markers are produced on a Si-SiO_2 substrate using electron beam lithography.

3)Deposition of nanowires on the SiO_2 surface

We put a droplet of the suspension on a SiO_2 substrate and blow it dry with nitrogen gas. If the surface contained too many nanowires (more than 1 nanowire per 10 x 10μm^2) it is advised to dilute the suspension in more solvent.

4)Selection of nanowires using optical microscopy and scanning electron microscopy

Nanowires with a diameter larger than 20 nm can be easily seen using an optical microscope. By optical microscopy we select the best candidates for a device. Scanning electron microscopy (SEM) is then used to locate the Sn-CNT's on the SiO_2 surface and to measure their thickness. SEM settings with acceleration voltages of more than 5 keV allows as to ascertain that the multi-walled nanotube is completely filled with tin, since an empty tube gives a different contrast. The majority of the nanotubes are completely filled with Sn, have a length smaller than 1.5 μm and a diameter around 50 nm. For the nanotubes which are partially empty, the length of the empty space does not exceed 200 nm and is found in most cases at one of the ends of the nanotube. Inspection by secondary electron microscopy (and by TEM [4]) shows that the carbon walls from the multi-walles nanotube contribute about 10 nm to the total diameter. Therefore a 50 nm

nanotube contains a 40 nm diameter Sn nanowire. We use EBL to pattern the electrodes on top of a single Sn-CNT.

5)Electron beam lithography

We spin PMMA 950K (4% in ethyllactat-n-Butylacetat, AR-P 679.04 from ALL-RESIST GmbH) at 4000 RPM to obtain a 250 nm thick polymer layer and annealed it for at least one hour to remove the solvent. Using electron beam lithography we define the positions at which to produce the gold contact to the nanowire.

6)Argon ion etching and Ti/Au evaporation

Prior to the evaporation of metals we argon etch the nanotube at the places where the electric contacts will be made. By this the carbon of the multi-walled carbon nanotube is partially removed making it possible for the metallic probes (Ti, Au) to make direct (or indirect through a tunnel barrier) contact to the Sn wire. We used etching times between 13 and 75 seconds. We evaporate 1.2 nm of Ti as adhesion layer in an e-beam evaporating system at $1.0 \cdot 10^{-6}$ mbar and 160 nm of Au by thermal evaporation. During the e-beam evaporation the sample surface can reach temperatures which can exceed the melting point of Sn. Continuation of deposition of Au by e-gun evaporation for longer times has as consequence the complete melting of the Sn. By capillary effect the melted Sn moves outside the MWNT through the Ar etched parts of the nanotube. To avoid this, we are forced to evaporate the Au (160 nm) in another system by thermal evaporation for which the temperature during the process is far below the melting point of Sn.

7)Lift off and wire bonding

Lift off is done in acetone at a temperature of about 30 ^{o}C. We glue the sample to a chip carrier. Connection between the samples and the sample holders is made using ultrasonic wire bonding.

3.2.4 Fabrication of a graphene spintronic device

For the production of a graphene based spintronic device we need to proceed via the following steps:

1)Preparation of gold markers on a SiO_2 surface

The markers are produced on a Si-SiO_2 substrate using electron beam lithography. The Si is highly doped (n, 0.0015-0.007 Ωcm) and the SiO_2 has a thickness of 500 nm.

2)Cleaning of the SiO_2 surface using oxygen plasma etching

We remove the organic remains on the SiO_2 surface using oxygen plasma etching (time: 3 minutes, power: 40W, O_2 flow: 9 sccm, pressure: 9 mbar).

3)Deposition of graphene on the SiO_2 surface

We use high quality Highly Oriented Pyrolytic Graphite (HOPG) as basic material for the graphene spintronic devices (grade ZYB). Studies show that the grade ZYA HOPG from GE Advanced Ceramics has substitutional impurities of no more than 30 ppm [5]. Note that heating the highly crystalline material to temperatures close to 2500°C in a controlled environment (in vacuum, or inert atmosphere like N, Ar, or He), should reduce the amount of impurities by at least a factor of 10. This can be concluded since this cleaning procedure is used as a purification step to obtain ultrapure Kish graphite samples [6].

Kish graphite is separated from kish, a byproduct of the steal industry, which is a mixture of graphite, desulfurization slag, and iron. Several cleaning procedures are used to remove the contamination from kish graphite, including acid treatment in HF and HCl. Ultrapure kish graphite is obtained by heating the material to temperatures higher than 2000°C resulting to impurity levels of less than 3 ppm [5]. For graphene electronics scientists prefer to use graphite material containing large graphite crystals and containing as less as possible impurities. Kish graphite for example contains crystals as large as several cm^2, impurity levels less than 3 ppm and give graphene layers having mobilities as high as 2 10^5 cm^2 V^{-1} s^{-1} [7]. Natural graphite is another example of graphite containing crystals as large as kish graphite. The situation is different for HOPG material. Depending on the grade of the HOPG material, it can have small graphite crystals ($\sim \mu m^2$) for the lowest grade, up to 1 cm^2 for the highest grade. The amount of impurities is usually less than 30 ppm [5]. For future experiments we have purchased all three grades of HOPG from GE Advanced Ceramics (grades ZYA, ZYB and ZYH), the highest grade HOPG from SPI (quality comparable to the ZYA grade of GE Advanced Ceramics) and kish graphite from Covalent Materials Corporation.

Deposition of the graphene layers on the SiO_2 surface is done using the mechanical exfoliation technique [8]. For this we press the sticking side a scotch tape on the 1 x 1 cm^2 HOPG sample surface. Pulling the tape away from the HOPG results in cleaving the HOPG. The freshly cleaved surface on the tape is now pressed strongly on the SiO_2 substrate, for this we use a rubber eraser. A rubber eraser is flexible and distributes the pressure on a large part of the substrate, by this we avoid damaging the SiO_2 surface.

4)Selection of a graphene layer

We use optical microscopy to select the graphene layer from multilayer graphene (see next section). Atomic force microscopy and in particular Raman spectroscopy is used to distinguish a single layer of graphene from a double layer.

5)Aluminum oxide layer

We evaporate a 0.6 nm thick Aluminum layer on the sample surface at ultra high vacuum conditions and at liquid nitrogen temperature. We oxidize it to produce a 0.8 nm thick Al-oxide layer.

6)Electron beam lithography

We spin PMMA 950K in such a way as to obtain a 140 nm thick polymer layer and anneal it for at least one hour to remove the solvent. Using electron beam lithography we define the positions at which to produce the ferromagnetic contacts on the graphene layer.

7)Lift off and wire bonding

Lift off is done in acetone at a temperature of about 30 ^{o}C, we dry the sample using nitrogen gas. We glue the sample to a chip carrier. Connection between the sample and the sample holder was made using ultrasonic wire bonding.

3.3 Selection of graphene flakes

We use optical microscopy to select the graphene flakes from the multilayer graphene. This selection is possible because a single layer of graphene gives a much smaller contrast with respect to two or more layers of graphene. Successively, the flakes are investigated by Atomic Force Microscopy (AFM). In this step we select the layers having a thickness smaller than 0.5 nm corresponding to a single graphene layer.

3.3.1 Optical microscopy

A single layer of graphene can become visible to our eye under an optical microscope just by choosing the right substrate and right light filters for the microscope. The optimum parameters can be found by modeling the optical response of visible light incident on a single layer of graphene on top of a substrate. The model calculations presented in this section are based on the experimental and theoretical

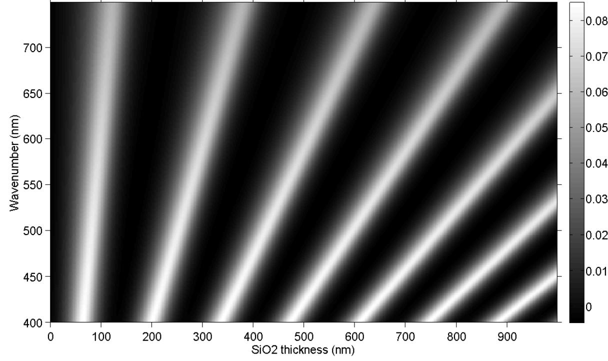

Figure 3.3: Contrast of a single layer of graphene on a Si/SiO_2 substrate as function of the thickness of the oxide layer and the wavelength of light. The contrast defined by eq. 3.1 can have a minimum of zero (black) up to a maximum of 8 % (white). For a 500 nm oxide we obtain a maximum contrast of 8 % when blue or green light is used.

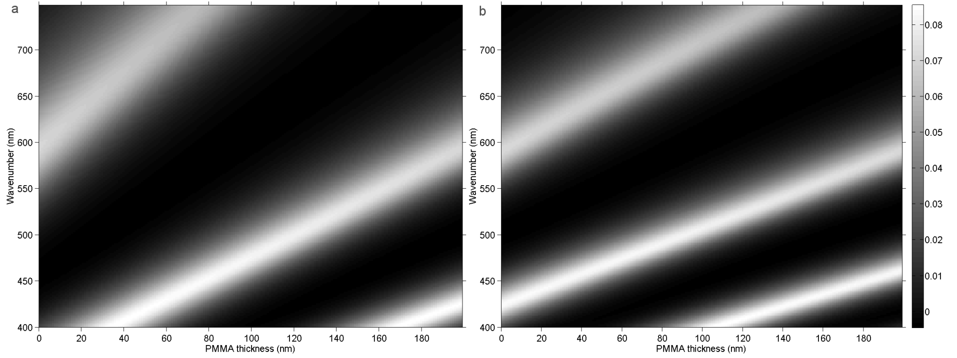

Figure 3.4: Contrast of a single layer of graphene on a Si/SiO_2/PMMA substrate as function of the thickness of the PMMA layer and the wavelength of light. a) For a 300 nm thick SiO_2 layer we obtain maximum contrast for a 100nm thick PMMA layer using blue light. b)When we use a 500 nm thick SiO_2 layer we obtain the highest contrast for a 70nm thick PMMA (blue light).

results found in Ref. [9]. We start with a graphene layer on top of a Si/SiO_2 substrate where the Si is semi-infinite in thickness and the SiO_2 has a thickness d_{SiO_2}.

The model contains 4 media with different optical properties, the first one is air, following a graphene layer, SiO_2 and the Si layer. Air has a refractive index close to one. The complex refractive index of graphene is $n_{grap} = 2.6 -$

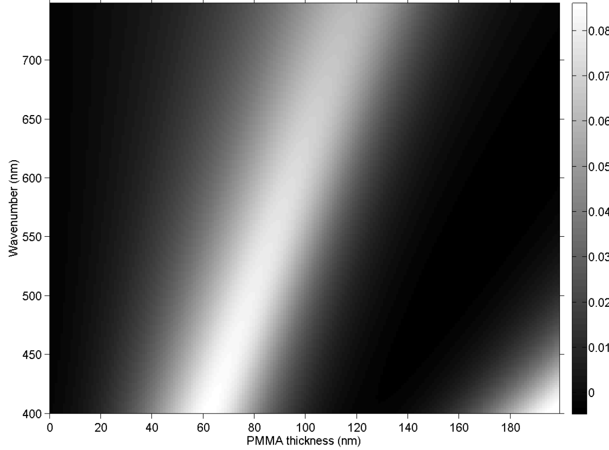

Figure 3.5: Contrast of a single layer of graphene on a Si/PMMA substrate as function of the thickness of the PMMA layer and the wavelength of light.

$1.3i$, of SiO_2 $n_{SiO_2} = 1.451 + 0.1654exp(-\lambda/182)$ and of Silicon $n_{Si} = 3.78 + 213exp(-\lambda/85nm) - i*(0.006 + 71452exp(-\lambda/33nm)$, where λ is the wavelength of light in nm.

The contrast in this system is given by the relation:

$$C = \frac{I(n_{SiO2}) - I(n_{grap})}{I(n_{SiO2})} \tag{3.1}$$

where $I(n_{grap})$ is the intensity of reflected light at a place where graphene is present and $I(n_{SiO_2})$ the intesity where there is no graphene. This intensity is given by the relation $I = r_{tot} r^*_{tot}$. For normal light incidence from air onto the graphene layer we have:

$$r_{tot} = \frac{r_{12} + r_{234} e^{-2\phi_2}}{1 + r_{12} r_{234} e^{-2i\phi_2}} \tag{3.2}$$

$$r_{234} = \frac{r_{23} + r_{34} e^{-2i\phi_3}}{1 + r_{23} r_{34} e^{-2i\phi_3}} \tag{3.3}$$

Furthermore, r_{ij} (i,j: 1...4) is the relative index of refraction, given by:

$$r_{ij} = \frac{n_i - n_j}{n_i + n_j} \tag{3.4}$$

ϕ_i is the phase shift and is given by $\phi_i = 2\pi n_i d_i / L$.

For a 300 nm thick SiO_2 layer we find the best contrast for light in the green range (Fig. 3.3) Blue and green light give the best contrast for a 500 nm thick SiO_2 layer. Note that a maximum contrast of 8 % is expected for a single layer. Our

model predicts a contrast of about 16 % for a double graphene layer. Experiments show indeed that this is the case, however, the spread in the contrast values is found to be big (Fig. 3.6).

The minimum contrast necessary to be visible to the human eye is found by performing simulation measurements on an original CCD picture of an oxide surface (500 nm SiO_2). A drawing program (paint shop pro) is used to measure the noise level in the picture. We found a noise level which corresponds to contrast fluctuations of about 1 %. Since the noise level is so high a graphene layer placed directly on top of a Si surface (no SiO_2) is not visible as the contrast is only -0.3%. To become visible we need a contrast of at least $\pm 1\%$. Selecting a 2 x 2 μm^2 area on the CCD picture and increasing the contrast of this area by 1 % shows that it is indeed visible in the current noise level. Our model shows that we can increase the contrast of the graphene layer on top of the Si surface by a factor of 3 just by spinning a thin layer of PMMA on top of the sample. For this the PMMA thickness has to be 90 to 100 nm thick (visible for L = 575 to 625 nm). A contrast of -1% is not large but it could be just enough to see a single layer under the assumption that we use optimized microscope and digital camera settings. The same trick can be used when the substrate is GaAs. A contrast of -0.4% is found at L = 450 nm for a graphene layer on GaAs. Spinning a layer of PMMA having a thickness of 60 to 80 nm should give a contrast between -1 to -1.2%.

Perhaps, a better way to find a thin layer of graphite on a substrate like Si or GaAs is the following. Spinning first a PMMA layer on top of Si of about 80 nm thickness and putting then graphene on top of it. The contrast is in this case about 7% when green light is used. Removal of the PMMA can be done in two different ways: a) Heating the sample to 300 ^oC for more than 3 hours in a Ar/H_2(95%/5%) environment. The hydrogen breaks apart the PMMA molecules is smaller pieces which evaporate away at 300 ^oC or b) First break down the PMMA molecules to smaller pieces by exposing it with a EBL beam (or using UV light) and afterwards heat up to 300 ^oC for several hours in a Ar/H_2(95%/5%) environment.

A graphene layer on top of PMMA should also allow us to produce in a relatively easy way a free standing graphene flake on top of a Si/SiO_2 substrate. Crucial for this experiment is to be able to observe a graphene layer by optical microscopy. The contrast of the graphene layer on PMMA can be found by modifying the model to incorporate one more layer (a PMMA layer between the SiO_2 layer and the graphene layer). We replace r_{234} with r_{2345} in equations 3.2 and 3.3, replace r_{34} with r_{345} in equation 3.3 and use the relation:

$$r_{345} = \frac{r_{34} + r_{45} e^{-2i\phi_4}}{1 + r_{34} r_{45} e^{-2i\phi_4}} \tag{3.5}$$

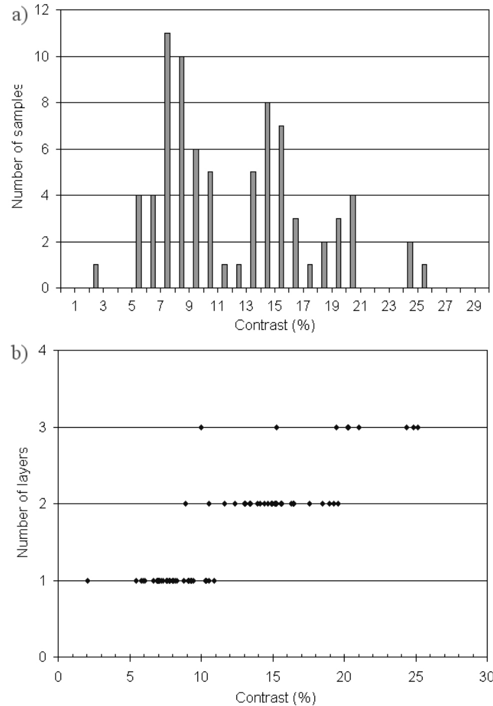

Figure 3.6: Contrast of 82 graphite layers on top of a 500 nm thick SiO_2 substrate. A optical microscope was used (green filter) and CCD images were taken. The contrast analysis from the images was calculated using eq. 3.1 and was performed by 3 students (each one investigated $\sim$1/3 of the 82 data points) a) A contrast plot containing all 82 graphite layers shows a clear accumulation of contrast values around 8 % and 15 % corresponding (as predicted by the model) to a single and a double layer graphene, respectively. b) Since a graphite layer with the weakest possible contrast corresponds to a single layer graphene and because increasing the number of layers results to a steplike increase in contrast, it is possible to guess the number of graphene layers each graphite layer contains. We asked the students to guess the number of graphene layers (y-axis) in each graphite layer by optical inspection and before the calculation of the contrast (x-axis). Two data points from the double layer graphene (31 data points) have a contrast found in the range in which the contrast of a single layer of graphene (39 data points) is predicted. Therefore using this type of selection and defining the contrast of a single layer to be below 10% (threshold) already gives a 5 % uncertainty. The uncertainty can be minimized almost to zero by setting the threshold value at 8%.

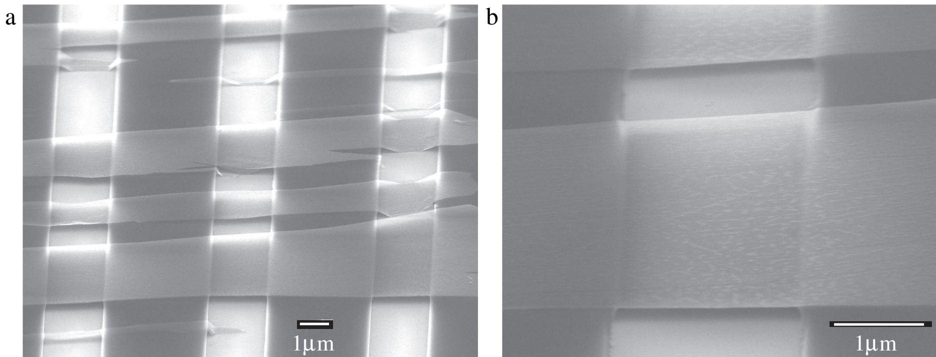

Figure 3.7: Free standing graphite. a) PMMA pillars of 70 nm thickness hold the graphite pieces suspended over 2 μm length. Electron beam lithography exposure is used to define the 2 μm width bridge and afterwards, development in IPA/MIBK is performed to create it. b) A 2 x 2 μm free standing flake on which some PMMA remains are visible

The media are in this case: air(1), graphene(2), PMMA(3), SiO_2(4) and Si(5). Using green light, the highest contrast (8%) is found for a 100 nm thick PMMA layer on top of a 300 nm thick SiO_2 layer (Fig. 3.4 a) The contrast in case of a 500 nm thick SiO_2 substrate is depicted in Fig. 3.4 b. A proof of principle is depicted in Fig. 3.7 in which we show free standing graphite layers on top of SiO_2. The procedure is straightforward. We spin PMMA (950K) on a 500 nm SiO_2 substrate in such a way that we obtain a 70 nm thick PMMA layer. After annealing it for 1 hour at 170 ^{o}C we use the mechanical exfoliation technique to produce graphene flakes on the PMMA. An optical microscope is used to select the graphite flakes having the smallest contrast, flakes containing only several graphene layers. We expose the area at which we would like the graphite to become free standing with a 100μC/cm^2 dose of 10keV electrons and we develop using a 1:3 ratio MIBK:IPA developer. After development we obtain free standing graphite flakes which are supported by 70 nm thick PMMA pillars (the non exposed PMMA). We did not produce a working free standing graphite electronic device. For this we need several crucial steps. The 950K PMMA should be free from solvent (anicole) and therefore should be annealed for at least 12 hours at 170 ^{o}C. After depositing the graphite on the 950K PMMA we need to spin a PMMA/MA layer and bake it for $\sim$10 minutes at 170 ^{o}C. The area at which we would like to produce a metallic contact to the graphite flake needs to be exposed with a dose high enough to break the PMMA/MA polymer but not the 950K PMMA. This contact will become free standing and therefore needs support pillars from both sides (free standing bridge) to the SiO_2. Good electrical contacts can be produced by thermal evaporation of

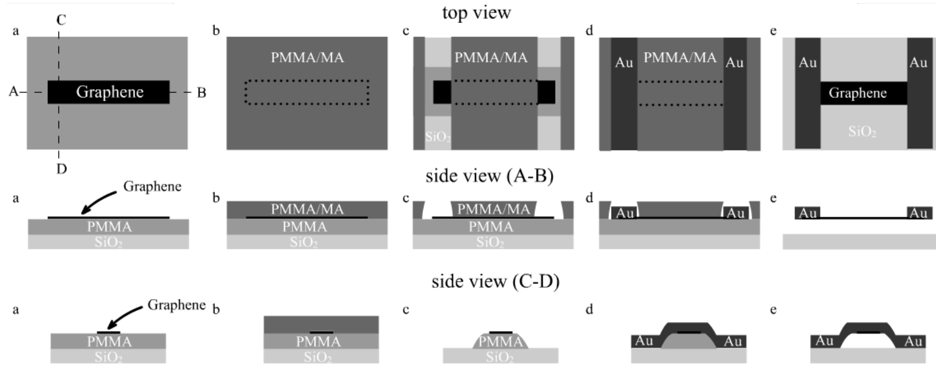

Figure 3.8: Creating a free standing graphene device. a)Single layer of graphene on 70 nm PMMA, b)Covering the sample with a thick layer of PMMA/MA(∼200nm), c)Defining the contacts after development. We use the minimum possible dose necessary to expose the PMMA/MA layer on top of the graphene layer. Far away from the graphene layer we use a high dose, enough to expose both the PMMA/MA and the PMMA 950K layer. d)Evaporation of Cr/Au contacts. A strong Au bridge it possible when the total electrode thickness is comparable to the PMMA thickness. e) A free standing graphene flake after lift off. Heating up the sample to 300 ^{o} C in a H_2/Ar (5%/95%) environment for 1 hour should clean up all PMMA remains on the graphene flake.

2 nm Cr and 150 nm of Au.

3.3.2 Raman Spectroscopy

Raman spectroscopy has been successfully used to characterize the electronic properties of single wall nanotubes [10]. The past two years Raman spectroscopy has also been proven to be a very powerful tool to distinguish a single graphene layer from several layers [11]. The amount of doping and the quality of a graphene layer can also be investigated by this technique [12]. In general, a Raman spectrum shows two intense peaks positioned at ∼1580 cm^{-1}(G band) and ∼2700 cm^{-1}(2D band) [13].

The G band is a standard Raman signal arising from the E2g in-plane vibration at the Brillouin zone centre of the carbon atoms [14]. The D band from the defect mediated zone-edge phonons. The 2D band comes from the second order resonant Raman scattering from zone boundary K+ΔK phonons. This band is used to distinguish single and multi- layer samples. Graphene has a sharp, single 2D peak (Full Width Half Maximum (FWHM) ≃30 cm^{-1}) in contrast with graphite and

few-layers graphene which show a broad peak [11]. First experiments showed that the G peak position or the intensity ratio of the 2D to the G peak I(2D)/I(G) could be used to estimate the number of layers, however further investigation proved that this is wrong [12]. The problem is that the spread in those parameters on a single layer for example far exceeds that assigned to the increase of number of layers. A very important Raman peak is the D peak (1350 cm^{-1}) which originates from the breathing modes of sp2 atoms and requires a defect for its activation. The D line is relatively strong with respect of the other lines in case the graphene layer has a lot of defects. Absence of this peak is a good indication of a good quality graphene flake.

The Raman data in figure 3.9 are recorded using a laser excitation of 532 nm. The Raman signature of a single layer clearly differs from layers containing two or more graphene flakes. The graphene 2D line is very narrow (32 cm^{-1}FWHM) compared to the 2D Raman line of a multilayered graphene flake (>60 cm^{-1}FWHM), in agreement with other studies [11, 12, 15]. In Fig. 3.9b we present the G band, which for this sample shows a single peak for a graphene layer and a double peak for multilayered flakes. Note that this spectrum is an exception since multilayered graphene flakes usually show a single peak with a width similar to the peak of a graphene layer. Finally, a graphene layer deposited on a 500 nm thick SiO_2 substrate was first characterized by Raman spectroscopy and afterwards investigated optically by making a CCD image of the layer (optical microscope with green filter). We obtained a contrast of 8.5% from the analysis of the CCD image which is close to the value calculated from the model developed in section 3.3.1 (8%, Fig. 3.3).

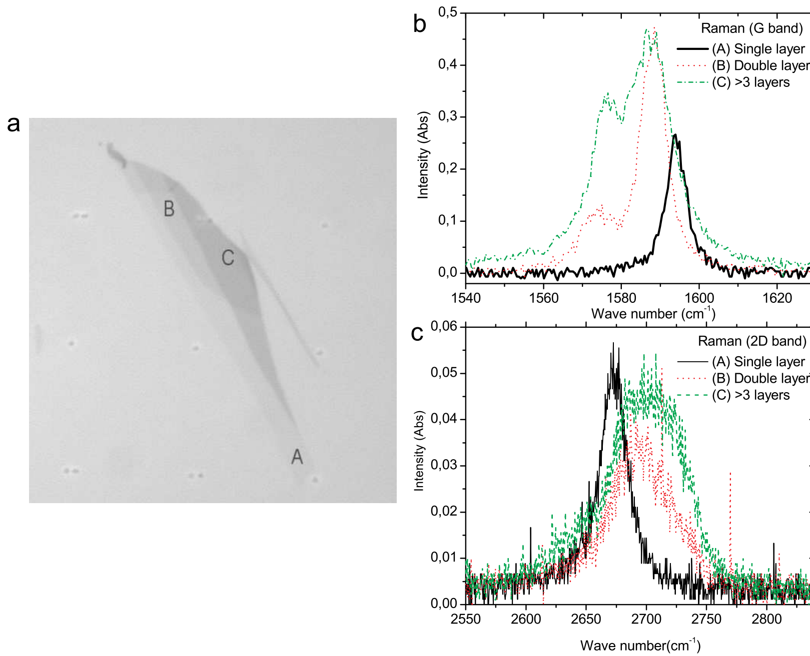

Figure 3.9: Raman specta using 532 nm excitation energy. a) Optical image of graphite on 500 nm SiO_2, at position (A) we have a single layer graphene, at (B) a double layer graphene and at (C) more than 3 layers of graphene. b) G band structure. Usually no distinction can be made between a single and a multilayered graphene flake, since they give a single peak with similar width. Here, remarkably, a single layer graphene shows a single narrow peak and the multilayered graphene flake a double peak. c) 2D band. The 2D peak of a graphene layer has a full width half maximum of 32 cm^{-1} which is narrower than multilayered flakes. This difference is used to distinguish a graphene layer from multilayered graphene flakes [11].

3.3.3 Atomic Force Microscopy

In our experiments we use atomic force microscopy in the tapping mode [16](Fig. 3.10). Here a cantilever-tip ensemble is exited to its resonance frequency. An electronic circuit measures the changes of the amplitude when the tip is attracted or repelled by the investigated sample surface. The changes are used as feedback parameters in such a way that the sample topography can be imaged. For the case of a graphene flake on a SiO_2 surface great care has to be taken on the different types of force which a cantilever-tip can sense. Van der Waals, adhesion and capillary forces are some examples.

We should take into account that a water film can be present inbetween the graphene flake and the SiO_2 surface during the sample fabrication which in our case is always done in air (humidity 55 - 70 %). Investigation of organic pentacene deposited on SiO_2 by S. Wo *et al* [17] shows that if an interfacial water layer is initially present on the SiO_2 substrate then this has a thickness of about 0.75 nm. This water layer remains at the interface after the deposition of a pentacene thin film. Also care has to be given to the hydration layer: The hydration layer is a general phenomenon that occurs at hydrophobic surfaces. It consists of a low-density water layer with a thickness of $\sim$0.15 nm in contact with the hydrophobic surface. Pentacene and graphene are hydrophobic and therefore a hydration layer is expected to form at its interface with water. Also, a water layer (0.7 - 1.1 nm) has been observed on the free surface of pentacene after sufficient exposure in air [17].

We deposit the graphite flakes on the SiO_2 layer immediately after strong O_2 etching which cleans up about 1 nm of PMMA remains on the surface. As graphene and pentacene have similar structure (hexagonal carbon lattice) we can expect the same results for graphene on SiO_2 as for pentacine on SiO_2. If water is only present on the SiO_2 surface then the AFM should give a thickness of about 0.45 nm, being the thickness of graphene (0.3 nm) plus the hydration layer. If now we have also water on the graphene layer then AFM should give a thickness of 1.1 to 1.5 nm making it us impossible to distinguish a graphene layer from multi-layers. If no water is present at all then a thickness of about 0.3 nm should be measured. We have to note that when the cantilever-tip comes too close to the surface then a liquid bridge may be formed between the tip and sample covered by water. This liquid bridge results to an attractive force which changes the amplitude of the tip in a different way than a van der Walls force. This problem can be solved by choosing a large tip amplitude in such a way that the distance between the tip and the water film is too large to result to a liquid bridge. Great care has also to be taken when no water is present. If we use small cantilever amplitudes then a false AFM image is produced as the tip interacts different to the hydrophillic SiO_2 than to the hydrophobic graphene. Solution is here again

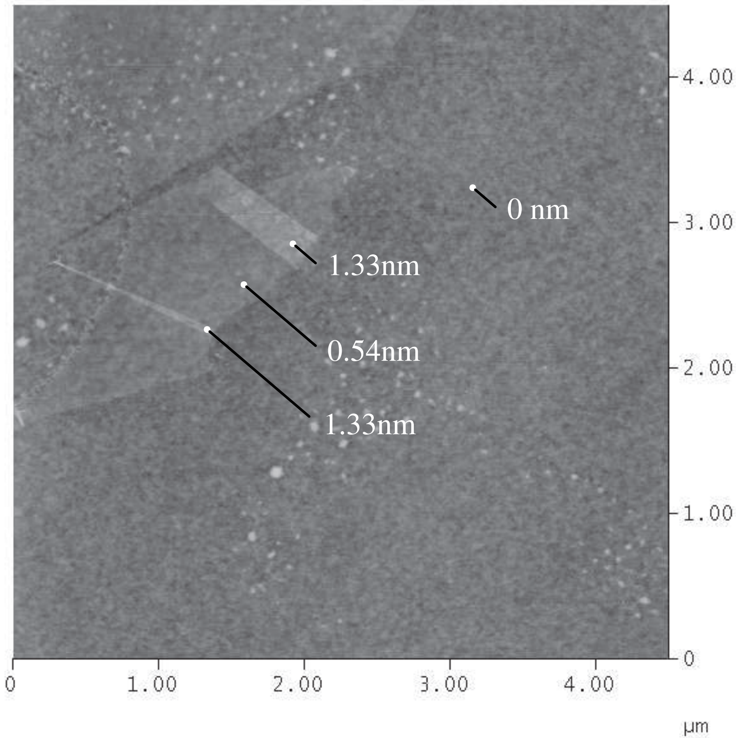

Figure 3.10: Atomic Force Microscopy of a single layer of graphene on SiO_2. A double folding of the graphene (= 2 x graphene thickness) results to a step height of $\Delta h = 1.33 - 0.54nm \approx 0.8$nm. The distance of the top of the graphene layer to the SiO_2 surface is 0.54 nm.

to use large cantilever amplitudes.

3.4 Electrical characterization setup

After completion of the device fabrication we glue the sample on a 16 or a 24 pin sample holder using Oxford Instruments varnish. Connection between the samples and the sample holders is made using ultrasonic wire bonding. We connect the sample to a resistance R and to pi-filters at room temperature (1 kΩ resistance and 10 nF capacitance). The filters not only reduce the pick up noise but also extend the lifetime of our devices, due to the fact that they cut out high frequency and high amplitude voltage spikes from the environment (Fig. 3.11). All measurements were done using the lock-in technique. The applied AC current on the sample has a sinusoidal shape at a frequency between 4 - 300 Hz. The

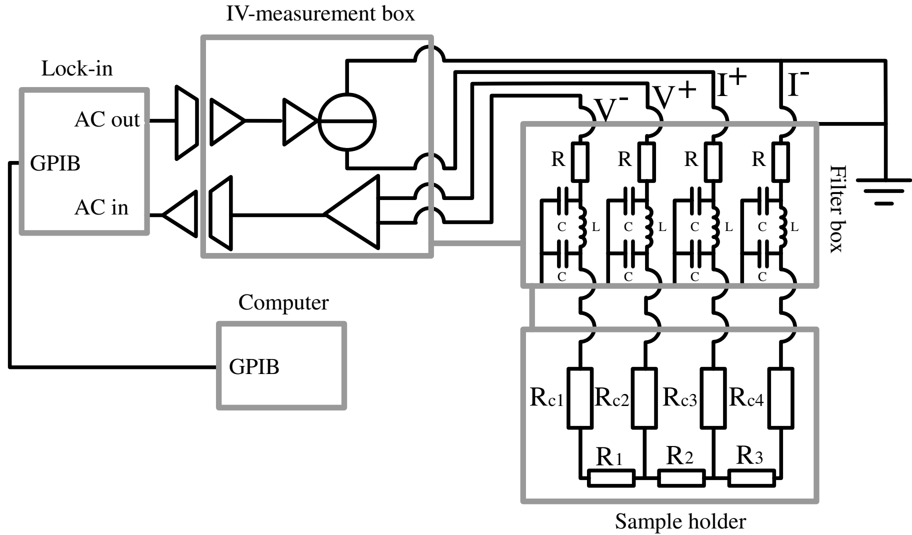

Figure 3.11: Example of a non-local 4 probe measurement. A Lock-in instrument produces an *ac* voltage ('AC out'). This voltage is translated to an *ac* current in the IV-measurement box. The amplitude of the current can be controlled by the user (from several pA up to 1 mA). The current passes through pi-filters in the filter box. After the filter box we have the sample holder. The electrical current passes trough a part of the sample, R_3, and through the contact resistances R_{c3} and R_{c4}. The voltage drop V^+ - V^- measured on the sample is amplified in the IV-measurement box. The amplification factor can be set to a value 10^n, with n = 0,1,2..5. The output voltage is fed back to a lock-in amplifier. Here the measured voltage is phase locked to a reference signal, which in this case is the frequency of the 'AC out'

detected signal is phased-locked with the applied signal. Since in our experiments the voltage probes usually detect very small voltage differences, it is of importance to separate large voltage fluctuations induced by the environment. For this, the measured voltage is amplified using the common mode rejection mode, which filters out external voltage fluctuations. A room temperature magnet is used for spin transport measurements at room temperature. Measurements between 1.5 and 4.2 K have been performed using a dip stick which is immersed in a liquid helium cryostat. Before immersing the dip-stick in helium it can be connected to a turbo pomp. By this the pressure can be controlled, from 1 atmosphere down to a vacuum environment of about 10^{-4} mbar. We use a 6 Tesla cryostat for applying high magnetic fields on the graphene spintronic devices and a 1 T cryostat for suppressing superconductivity in the tin nanowire devices.

References

[1] W. M. Moreau, *Semiconductor Lithography*, (Plenum Publishing Co., New York, 1988)

[2] Mark A. McCord, Introduction to Electron-Beam Lithography, Short Course Notes Microlithography, 1999, SPIE's International Symposium on Microlithography 14-19 March, (1999)

[3] R. Krupke, *et al.*, *Science* **301**, 344 (2003)

[4] L. Jankovic, *et al.*, *Nano Lett.* **6**, 1131-1135 (2006).

[5] P. Esquinazi, *et al.*, *Phys. Rev. B* **66**, 024429 (2002)

[6] Y. Kaburagi, Y. Asano and Y. Hishiyama, *Carbon* **42**, Issue 15, 3266 (2004)

[7] K. I. Bolotin, *et al.*, cond-mat/0802.2389v1 (2008)

[8] A.K. Geim and K.S. Novoselov, *Nature Materials* **6**, 183 (2007).

[9] P. Blakea, *et al.*, *Appl. Phys. Lett.* **91**, 063124 (2007)

[10] S. Reich, C. Thomsen, and J. Maultzsch, *Carbon nanotubes: basic concepts and physical properties*, (Wiley- VCH, 2004)

[11] A. C. Ferrari, *et al*, *Phys. Rev. Lett.* **97**, 187401 (2006)

[12] C. Casiraghi, *et al.*, Cond mat:/0709.2566v1

[13] A. C. Ferrari, *et al.*, *Phys. Rev. Lett.* **97**, 187401 (2006)

[14] Anindya Das, Biswanath Chakraborty and A.K. Sood, Cond mat:/0710.4160v1

[15] F. Molitor, *et al.*, Cond mat:/0709.3426v1

[16] R. Garcia, R. Perez, *Surface Science Reports* **47**, 197 (2002)

[17] S. Wo, B. Wang, *et al.*, *Jour. of Appl. Phys.* **100**, 093504 (2006)